C.2-9

Met Apps 1, 337–350 (1994)

The October–1987 floods in Catalonia: synoptic and mesoscale mechanisms

Clemente Ramis, *Geophysical Fluid Dynamics Group, Departament de Física, Universitat de les Illes Balears, 07071 Palma de Mallorca, Spain*

Maria C. Llasat, *Departament de Astronomia i Meteorologia, Universitat de Barcelona, 08028 Barcelona, Spain*

Ana Genovés and Agustín Jansà, *Instituto Nacional de Meteorología, Centro Meteorológico de Baleares, 07071 Palma de Mallorca, Spain*

A heavy rainfall event which produced floods in Catalonia (Spain) during October 1987 is presented. Convection was located over the same area for several days, producing up to 431 mm of rain (67% of the mean annual rainfall). The synoptic-scale pattern and forcing are studied using objective techniques, while mesoscale features are investigated with satellite imagery and subjective surface analysis. Strong quasi-geostrophic forcing for vertical motion was diagnosed at low levels while only a weak forcing was evident at 500 hPa. Convective and latent instability characterized the region during the period of heavy rainfall. Also, there was strong low-level moisture convergence combined with high values of precipitable water over the north-west Mediterranean Sea. Composite charts delineating the area covered by the indicated synoptic factors seem to be an effective tool for identifying the area where mesoscale focusing mechanisms became effective. Sub-synoptic analyses show that the main focusing mechanism was a quasi-stationary convergence line, located near the coast of Catalonia. This lay between the south-eastern warm and humid flow, caused by a weak low centred north of the Algerian coast, and the cold outflow from a mesohigh located in Catalonia and mainly originated by the orographic blocking of the Pyrenees.

1. Introduction

On the evening of 28 September 1987, heavy rainfall brought the dry Mediterranean summer to an abrupt end in the Catalonian region of Spain (see Figure 1 for location and Figure 2 for major geographical features). Heavy rainfall continued intermittently in Catalonia and southern France for the eight-day period ending 5 October 1987, but most of the precipitation fell during the last four days. Much of the coastal section of Catalonia was affected by flooding, resulting in road closures and disruption of the railway system. Sils Lake, which is located near the city of Gerona and which had been dry since the middle of the nineteenth century, overflowed its banks. By the end of the flood event, ten people had been killed and the damage in north-eastern Spain was estimated at 10^9 ECUs (from press information).

The Spanish Mediterranean region – Catalonia included – is often affected by heavy convective rain, specially during autumn. For example, during October 1982 an official observation at Alicante indicated 83 mm in one hour (García-Dana *et al.*, 1982) and in Catalonia, during September 1962, 110 mm was collected in one hour in Sabadell (Bennet, 1986). Moreover, most observing stations in the region have maximum recorded rainfall amounts of over 200 mm in 24 h in the autumn (Font, 1983).

Phenomenological and synoptic studies have been performed on Spanish Mediterranean flood cases (García-Dana *et al.*, 1982, among others), and some of them referred specifically to Catalonia (e.g. Llasat, 1987). These events typically are associated with the presence of a cold trough or a cut-off-low located at the south-west of the Iberian Peninsula; these produce south-westerly diffluent flow in the middle and high troposphere over the Western Mediterranean. At the lowest levels an easterly flow from the Mediterranean towards the Spanish coast provides warm and moist air to feed the convection.

Other studies have put the emphasis on the blocking over the North Atlantic by an anticyclone located over Central Europe (Alonso & Puigcerver, 1978; Llasat, 1987). More-recent studies have highlighted the influence of low-level 'Algerian' cyclogenesis, which causes

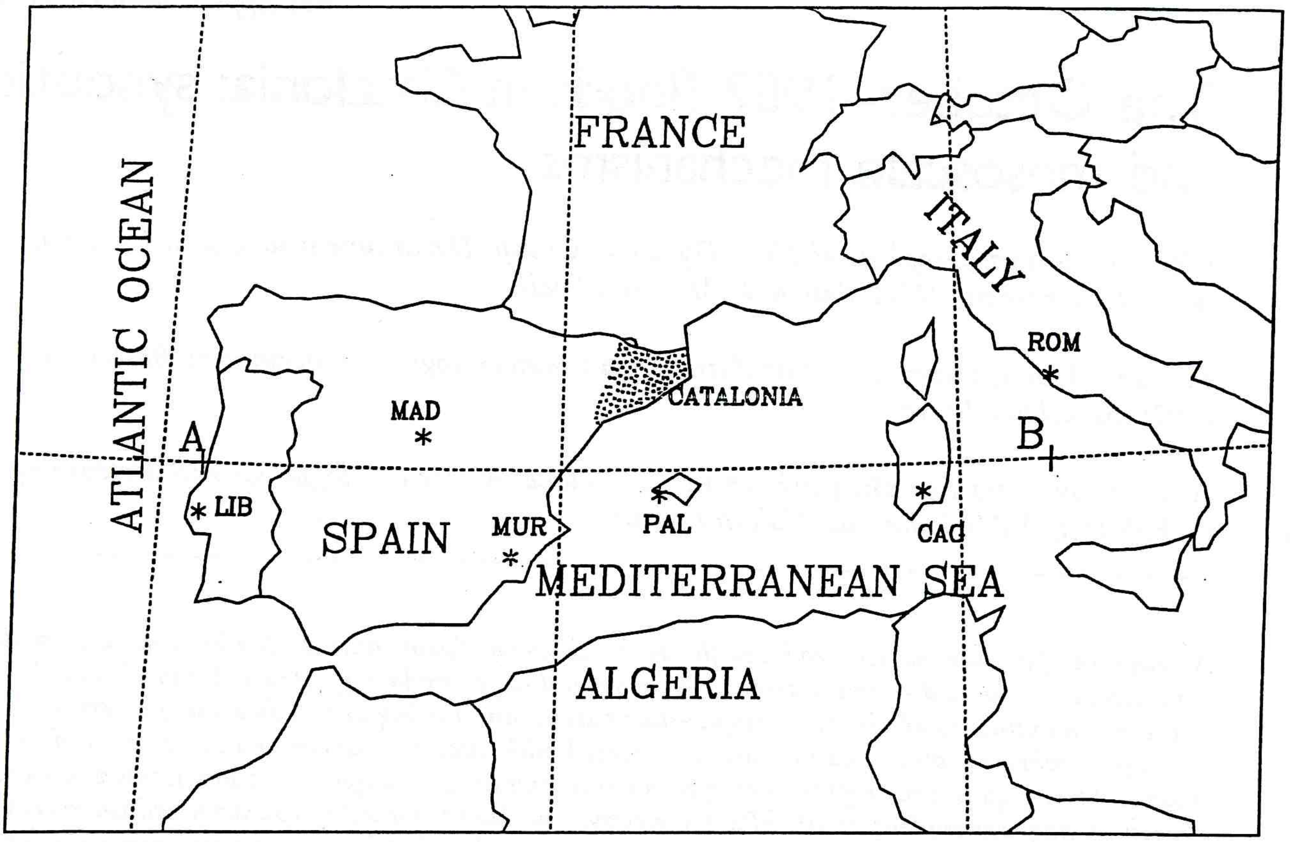

Figure 1. *Geographical location of Catalonia (dotted). The location of radiosonde stations used for cross-section A–B are indicated: Lisbon(LIB), Madrid(MAD), Murcia(MUR), Palma(PAL), Cagliari(CAG) and Rome(ROM).*

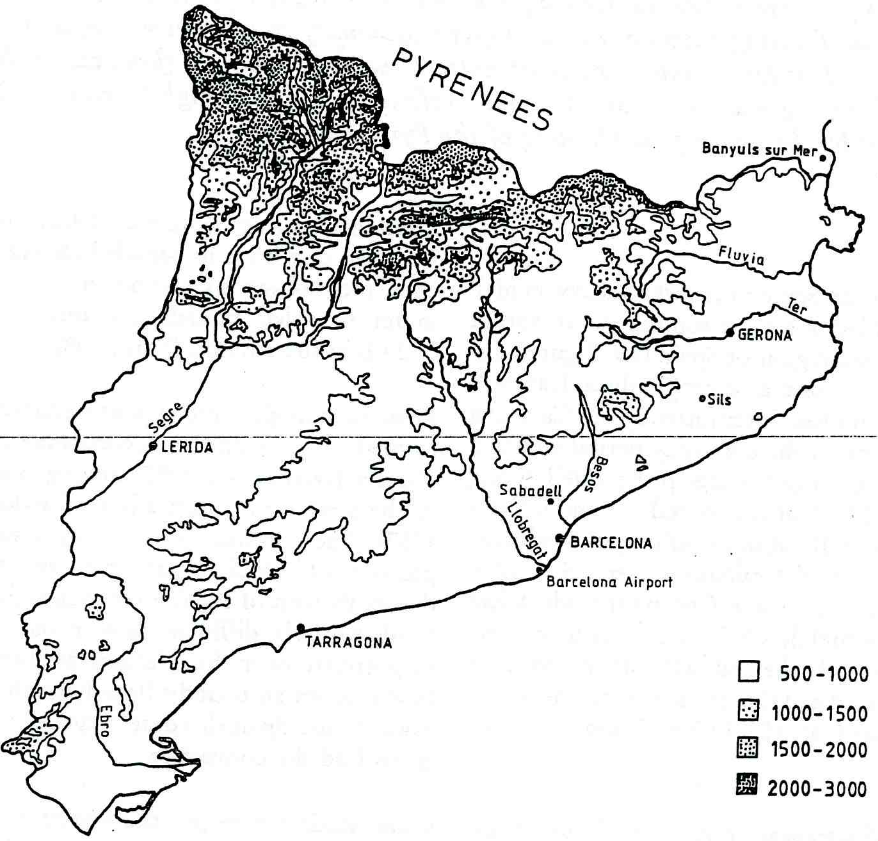

Figure 2. *Major geographical features in Catalonia. Contour interval for terrain height is 500 m. Some places mentioned in the text are indicated.*

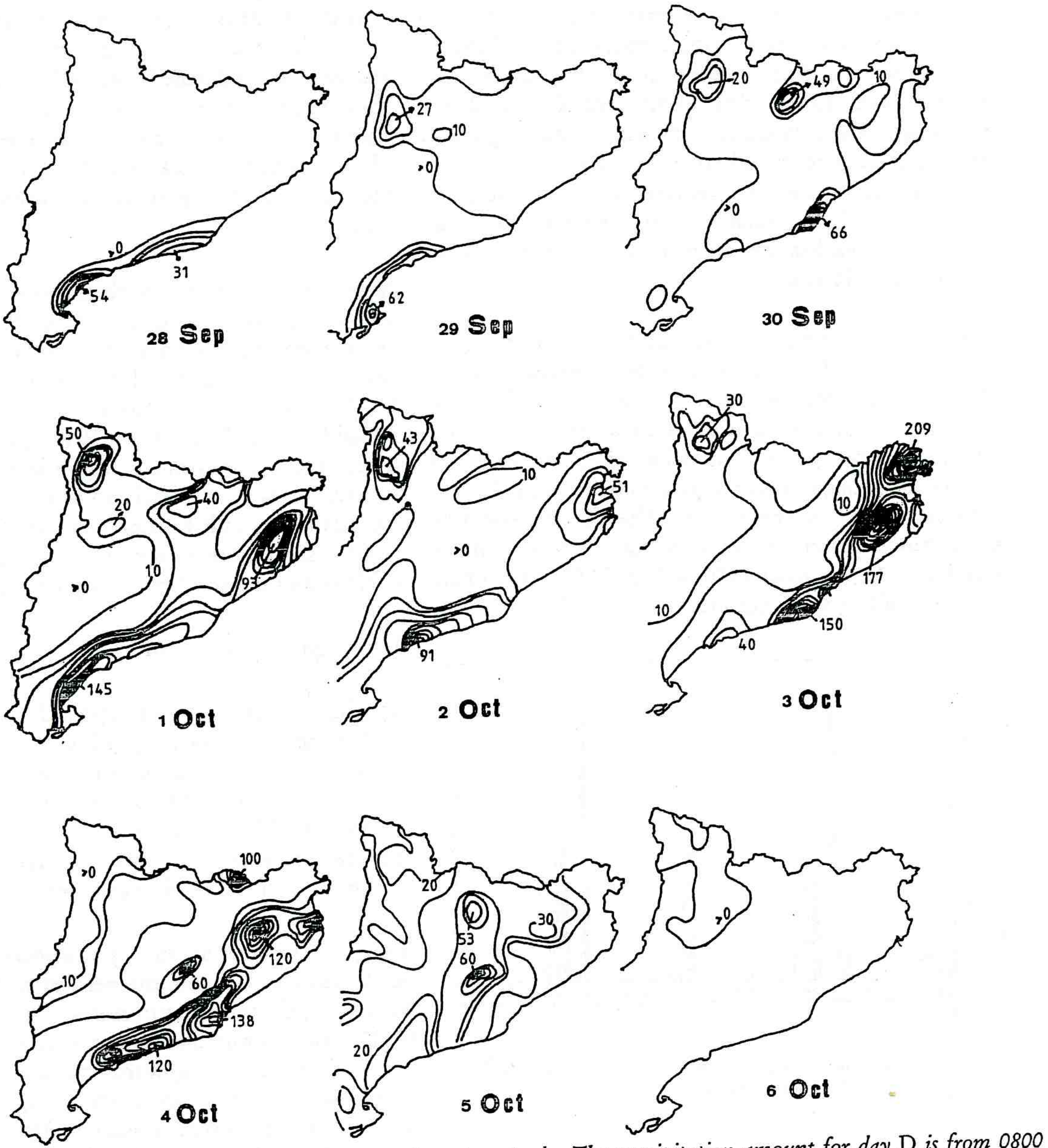

Figure 3. *Daily accumulated precipitation (mm) during the rain episode. The precipitation amount for day* D *is from 0800 UTC on day* D *to 0800 UTC on day* D+1.

convergence in the low-level flow (Jansá *et al.*, 1986), and the organization of the convection as Mesoscale Convective Systems (MCS) (Riosalido, 1990).

The purpose of this paper is to provide a detailed synoptic diagnosis and sub-synoptic examination of the meteorological causes of this heavy rainfall event. In so doing, we seek to add more-specific information to the general flash-flood scenario for Catalonia which has been identified in previous studies, through the determination of derived fields from the numerical products obtained by the Instituto Nacional de Meteorología (INM) of Spain and the mesoscale hand-analysis technique. In section 2 quantitative details about the event are given. Section 3 studies the synoptic scale setting, during the heaviest rain period. Section 4 deals with mesoscale aspects when deep convection was present. Finally, we summarize our conclusions in section 5.

2. The event

The description of the event is mainly based on the data from the 85 rain gauges in Catalonia and 20 in southern France. Most of them only provide measurements of 24-hour accumulated rainfall, though a few give continuous measurements.

What is unusual about this event is the repetition of quite heavy rain day after day, for several days, in the same zone, even in the same locality (Figure 3). Every day the largest precipitation amounts are located at or close to the coast, but at different places. Particularly important maxima occurred on 3 October at Gerona (209 mm) and on 4 October at Barcelona (138 mm). The southern part of France near Catalonia was also affected by heavy rain, with a maximum of 305 mm on 3 October at Banyuls sur Mer, the highest 24-hour precipitation during this event (see Figure 2 for locations). The maximum total rainfall was registered at Barcelona Airport, where 431 mm was collected in the eight-day period; this represents 67% of the mean annual rainfall. For such a short period this was the most important heavy rain event in the coastal zone of Catalonia in 50 years.

Figure 4 illustrates the hourly distribution of the rain. The data come from Hospitalet de Llobregat, located about five kilometres south of Barcelona. The total eight-day amount of precipitation at Hospitalet was 235 mm, certainly less than at Barcelona Airport, but significant enough to give a good indication of the distribution of the showers in time. This figure shows five main shower periods with the largest hourly accumulation being 33 mm from 1100 to 1200 UTC 4 October, 17.5 mm falling in 10 minutes.

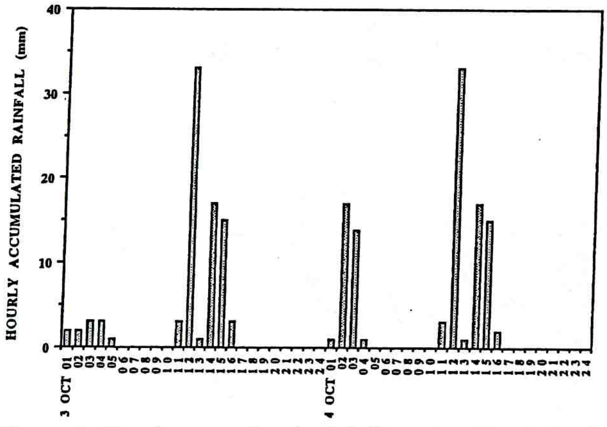

Figure 4. *Hourly accumulated rainfall (mm) at Hospitalet de Llobregat during 3 and 4 October.*

3. Meteorological setting

The forecast and the post-event analysis of convective weather has two phases. The first consists of identifying the characteristics of the synoptic-scale environment which are favourable to producing and sustaining convective storms. In the second, the smaller-scale features determining the localization of convective events within the favourable synoptic-scale environment should be identified (Rockwood & Maddox, 1988). McGinley (1986) indicates that the parameters that are necessary to produce convection with a potential for flash flooding area;

(a) synoptic scale upward vertical motion,
(b) unstable stratification,
(c) moisture, and
(d) low-level convergence.

From the point of view of Doswell (1987), diagnostics from synoptic weather maps can provide the 'dynamics' (quasi-geostrophic forcing) and part of the 'thermodynamics' (combination of moisture and stability), but a detailed study of the 'thermodynamics' should use data from upper-air soundings. Mesoscale phenomena, within an appropriate 'dynamic' and 'thermodynamic' background, represent the focusing mechanism that triggers the development of convective cells.

In this section we present the synoptic diagnosis of the convective event using geopotential height, temperature, humidity and wind components as generated by the limited area model (LAM) analysis system of the INM of Spain (Diaz-Pabón, 1988). Data values are available on a 0.91° (latitude/longitude) grid in the horizontal and standard pressure levels in the vertical. In addition we have used radiosonde ascents from six stations over south Europe and the Western Mediterranean (see Figure 1) for constructing vertical cross-sections and thermodynamics profiles.

The diagnosis consists of:

(a) The identification of upward quasi-geostrophic forcing (hereafter FQ), which forces upward synoptic-scale vertical motion, the moisture flux and the spatial distribution of convective instability from LAM analysis data.
(b) The more-detailed study of radiosonde ascents close to the zone of heavy rain.

The quasi-geostrophic theory is a powerful tool which can be used to estimate the vertical motion associated with synoptic-scale disturbances. Caracena & Fritsch (1983) pointed out that the synoptic-scale identification of areas of upward motion using quasi-geostrophic analysis can provide important guidance for nowcasting convective storms. Also, Barnes (1985), Durran & Snellman (1987) and Shou-Jun Chen *et al.* (1988) show that analysis of the FQ of vertical motion can provide short-term assistance with the prediction of heavy rainfall events. The convective (potential) instability can be an important factor for thunderstorm development if synoptic-scale vertical forcing is present (Iribarne & Godson, 1981). Also, the moisture convergence in a layer close to the ground over a convective area is a necessary mechanism to sustain deep moist convection rooted in the boundary layer (Barnes & Newton, 1986).

The FQ of vertical motion (FQ>0 for ascent) on isobaric surfaces has been calculated by using the Q-vector formulation of the ω-equation (see Hoskins & Pedder, 1980). For this purpose, the non-initialized geopotential height and temperature fields were filtered to eliminate short wavelengths by using the procedure described by Gomis & Alonso (1988).

3.1. Synoptic-scale overview

During the heaviest rain period the large-scale was changing slowly, so synoptic charts are presented only for half way through, namely 0000 UTC 4 October (Figure 5), and at the end of the event, 0000 UTC 5 October (Figure 6). The meteorological situation was characterized at 1000 hPa/surface (Figure 5(*a*)) by a low located to the north-west of the Iberian peninsula, which advected warm and humid Atlantic air over Spain, and an anticyclone located over Scandinavia, which extended its influence to the Western Mediterranean where it produced moderate winds and warm advection from the south-east. A weak trough north of the Algerian coast increased the winds in the northern part of the Western Mediterranean. At 850 hPa (Figure 5(*b*)) the pattern was very similar to that at the surface. The Scandinavian anticyclone extended its influence up to Africa and produced a moderate warm-air flux from the south over the Western Mediterranean. At 500 hPa (Figure 5(*c*)) a closed low was located over the surface low with a positively tilted trough to the west of Spain and a ridge over the Western Mediterranean where temperature advection was not present. At 500 hPa there was very weak cyclonic vorticity advection (CVA) over eastern Spain while at 300 hPa (not shown) the south-westerly jet stream associated with the low was located over the Iberian peninsula, so no upper dynamic forcing can be qualitatively identified close to Catalonia. Diagnosis of FQ shows that at low levels (850 hPa, Figure 5(*d*)) there was upward forcing over Catalonia and the gulf of Lyon but downward forcing over the gulf of Genoa and south of the Balearic Isles. Over the Western Mediterranean, FQ at 500 hPa was very weak, while more significant values were to the north-west of Spain and related to the cyclonic circulation.

A significant change in the synoptic pattern was observed at 0000 UTC 5 October. Figure 6(*a*) and (*b*) shows that a cyclogenetic process reactivated the Algerian trough, which appeared as a closed low at 1000 hPa and as a marked cyclonic circulation at 850 hPa. The wind from the south-east/south and warm-air advection became quite strong over the northern part of the Western Mediterranean. The Atlantic low moved to higher latitudes, and reduced its influence over Spain. At 500 hPa (Figure 6(*c*)) the Atlantic low had split into two centres, one located over the gulf of Cadiz and the other to the west of France; stronger winds at upper levels were over Morocco. The CVA became appreciable over south-eastern Spain but not very significant over the north-western Mediterranean. The Mediterranean cyclonic circulation at low levels

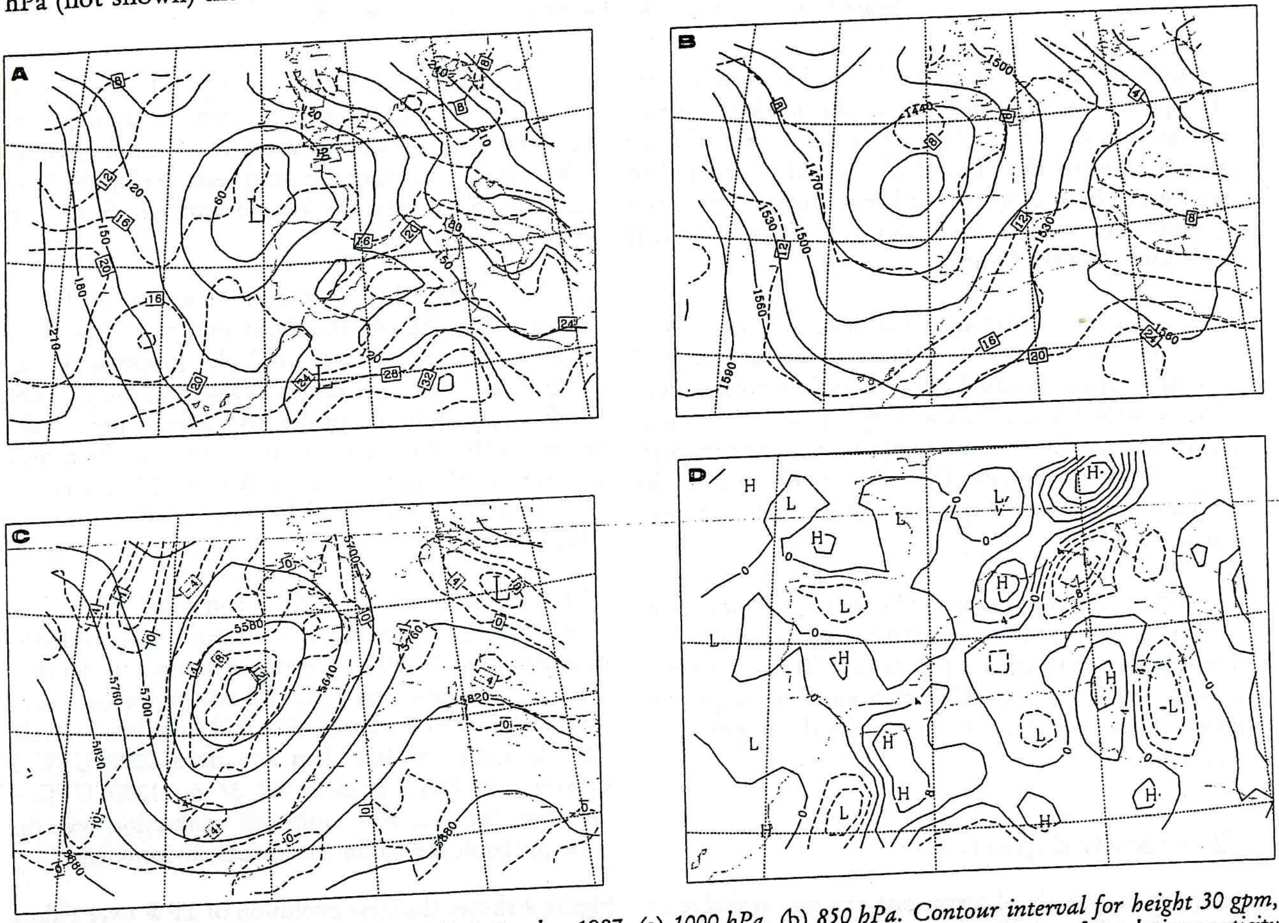

Figure 5. *Synoptic situation at 0000 UTC 4 October 1987.* (a) *1000 hPa,* (b) *850 hPa. Contour interval for height 30 gpm, for temperature 4°C.* (c) *500 hPa (height and relative vorticity). Contour interval for height 60 gpm, for relative vorticity $4\times10^{-5}\,s^{-1}$.* (d) *Quasi-geostrophic vertical forcing at 850 hPa. Solid and dashed lines indicate forcing of upward and downward vertical motion, respectively. Isoline interval 4×10^{-18} m kg^{-1} g^{-1}.*

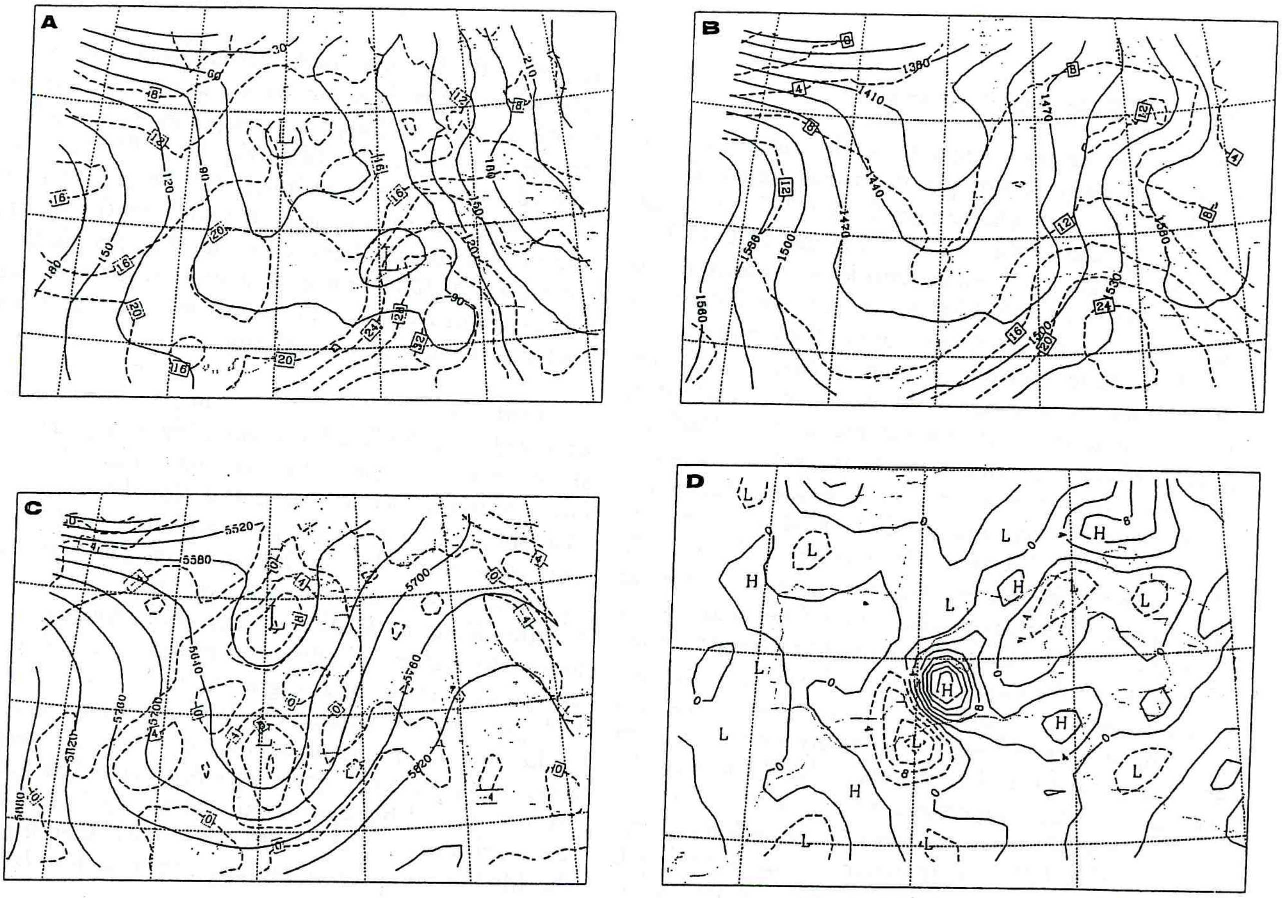

Figure 6. *As for Figure 5 but for 0000 UTC 5 October 1987.*

appeared as a strong dipole of FQ (Figure 6(*d*)), but the upward forcing continued to the north-east across a sharp zone to the north of Italy. At 500 hPa the greater upward FQ continued over Morocco and to the west of France, where the baroclinic wave structure is easily identified, but weak upward FQ was present over south-eastern Spain.

The cyclogenetic process at low levels led to the end of the heavy rain episode. The transport of low-level cold air eastward behind the low as it moved rapidly to the north stabilized the atmosphere over the Mediterranean. The circulation over Spain became progressively zonal throughout the troposphere, while the meridional flow was displaced towards Italy and central Europe.

These diagnostics indicate the existence, near and over Catalonia, of large-scale upward vertical forcing at low levels, associated with a significant differential thermal advection giving favourable conditions for the generation of weak static stability and the development of convection.

3.2. Instability diagnosis

Although upper-air observations are not available in Catalonia, Llasat (1987) has shown that radiosonde ascents from Palma (PAL, see Figure 1) are the most representative of atmospheric stability during heavy rain events in Catalonia. Moreover, since the wind at lower levels was from the south-east during the heavy rain episode, Palma was located upstream from Catalonia on this occasion.

The latent instability of an air mass can be studied by means of well-known instability indices or by calculation of the convective available potential energy (CAPE) (Weisman & Klemp, 1986) and the potential for flooding by means of the tropospheric precipitable water (TPW). Since no statistical study on the threshold value of the indices for the Western Mediterranean exists, the latent instability has been studied by means of CAPE.

The time evolution of CAPE and bulk Richardson number (Ri), as defined by Weisman & Klemp (1986), over Palma at 12-hour intervals is shown in Figure 7. The very rapid increase of CAPE was produced mainly by the entrance of warm and humid air at lower levels. The Ri values of less than 100 from 0000 UTC 3 October, with a minimum of 37 on 1200 UTC 4 October, indicate that multi-cell convection was the most probable development in that environment.

Figure 8 shows the time evolution of TPW over Palma and Murcia (see Figure 1 for location). The higher

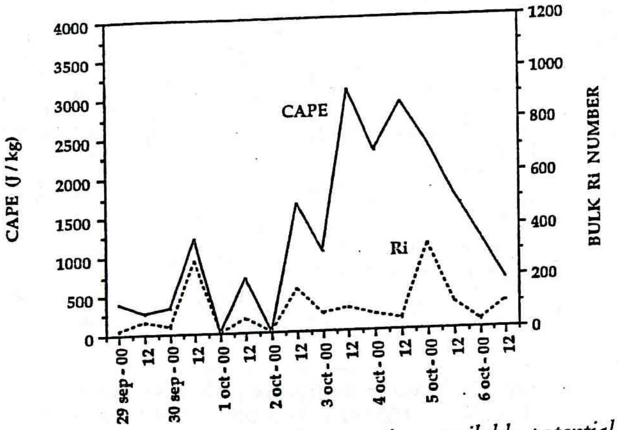

Figure 7. *Time evolution of convective available potential energy (CAPE) and bulk Richardson number (Ri) over Palma.*

values over Palma, up to 44 mm at 1200 UTC 4 October (180% of the normal value during the same time of the year, Ramis, 1976), were a consequence of moisture increase from the surface up to 500 hPa. This was confirmed by examination of the time evolution of potential temperature (θ) and equivalent potential temperature (θ_e) cross-sections (not shown). The important increase of TPW observed over Palma from 1200 UTC 3 October to 0000 UTC 5 October was not observed in Murcia. This result shows that the advection of humidity was modulated by the cyclonic circulation over the Algerian sea. The vertical profiles of temperature and dew point over Palma from 1200 UTC 3 October to 0000 UTC 5 October were typical of conditions preceding Type C thunderstorms in the USA (Barnes & Newton, 1986), which can develop heavy rain but not severe weather.

A zonal cross-section along 40° N (AB in Figure 1) at 0000 UTC 4 October is shown in Figure 9. The θ distribution indicates that abnormally warm air was located over the Western Mediterranean at all levels (Ramis, 1976). However, the θ_e distribution shows that the humid air was concentrated over Palma, where the convective instability was very strong. This instability could have been released by an upward displacement of the atmospheric column of only 200 m.

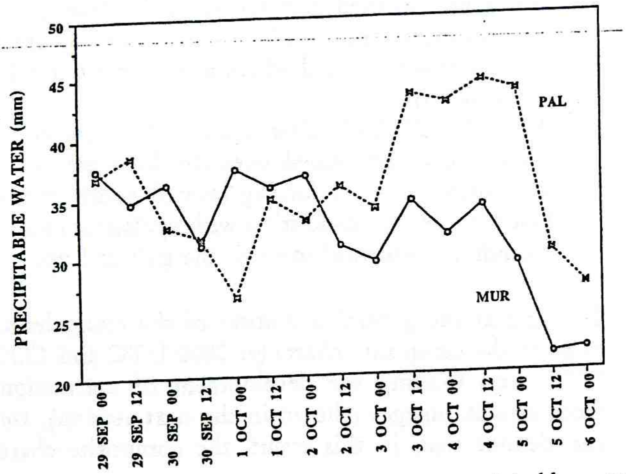

Figure 8. *Time evolution of tropospheric precipitable water (mm) at Palma (PAL) and Murcia (MUR).*

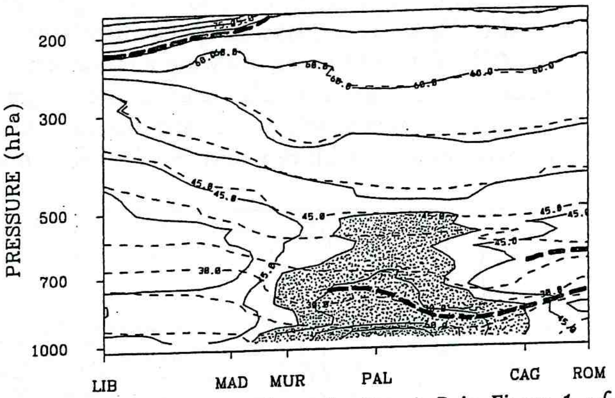

Figure 9. *Cross-section, along the line A–B in Figure 1, of potential temperature (dashed lines) and equivalent potential temperature (solid lines) at 0000 UTC 4 October. Contour interval is 5°C. Shaded zone highlights potential instability. Thick dashed lines represent inversions and tropopause. Distance from A to B is 1821 km.*

This analysis of radiosonde data indicates that the atmospheric structure over the Western Mediterranean was favourable to the development of deep moist convection. Moreover, a smooth distribution of the 'thermodynamics' can also be deduced from LAM analysis data. The temporal evolution of the spatial distribution of the difference of θ_e between 500 and 1000 hPa has been calculated and Figure 10 shows an example for 0000 UTC 4 October. Positive and negative values represent potential stability and instability of the layer, respectively. At 0000 UTC 2 October the potentially unstable air was located over Africa and south-west of the Western Mediterranean. By 0000 UTC 4 October the unstable air mass covered the Iberian peninsula and the Western Mediterranean, whereas stable air was associated with the anticyclonic circulation over France and Italy. During the final stage of the heavy rain episode, potentially stable air swept across the Iberian peninsula.

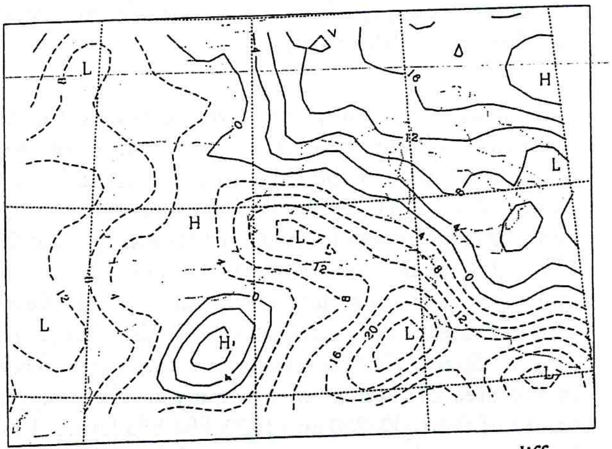

Figure 10. *Equivalent potential temperature difference between 500 and 1000 hPa at 0000 UTC 4 October. Solid and dashed lines represent positive and negative values, respectively. Contour interval is 4°C.*

Schwartz *et al.* (1990) use the surface θ_e as a surrogate for CAPE; high values of θ_e indicate large values of CAPE. Figure 11 displays the spatial distribution of θ_e at 0000 UTC 3 October, showing a maximum to the south of the Balearic Isles and a strong gradient towards Catalonia, which indicates the juxtaposition of two air masses with very different specific humidity.

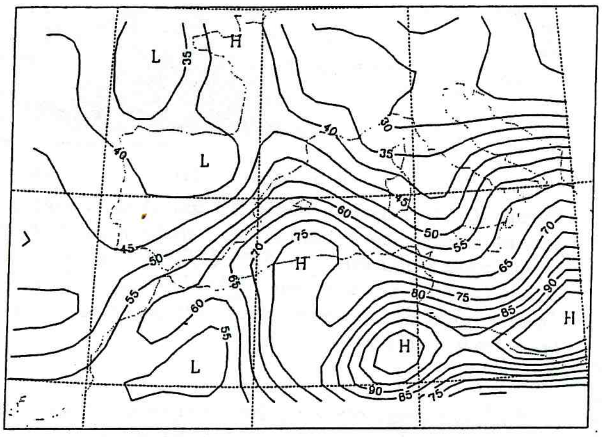

Figure 11. *Equivalent potential temperature at 1000 hPa for 0000 UTC 3 October. Contour interval is 5°C.*

3.3. Moisture flux divergence fields

The divergence/convergence of moisture in the layers 1000–700 hPa and 1000–850 hPa were calculated from the LAM analysis data. At 0000 UTC 2 October there was water vapour convergence in both layers over north-eastern Spain and divergence over western Spain. By 0000 UTC 4 October, moisture divergence covered most of the Iberian peninsula, with a maximum over Catalonia, while convergence was observed over the Western Mediterranean. Comparing these results with the spatial distribution of vertical velocity at 800 hPa deduced by the kinematic method, using the O'Brien (1970) adjustment (not shown), it is inferred that in the computation of the moisture divergence field the term including velocity divergence dominates the advective term. A similar result was obtained by Elsner *et al.* (1989) in the study of the flash flood of 6 August 1986 in Milwaukee, Wisconsin.

Following this result, we have calculated the time evolution of the divergence/convergence of water vapour at 1000 hPa and Figure 12 shows that distribution at 0000 UTC 4 October. The moisture convergence maximum was located over eastern Spain at 0000 UTC 2 October. In the next 48 hours the zone of convergence moved slowly eastward to the Western Mediterranean and Catalonia with divergence over most of Spain. That represents an important difference in the area of interest with respect to the integrated values of the 1000–700 and 1000–850 hPa layers. In the last stage of the event, at 0000 UTC 5 October, the water vapour convergence at 1000 hPa was very strong over the Western Mediterranean in agreement with the integrated values.

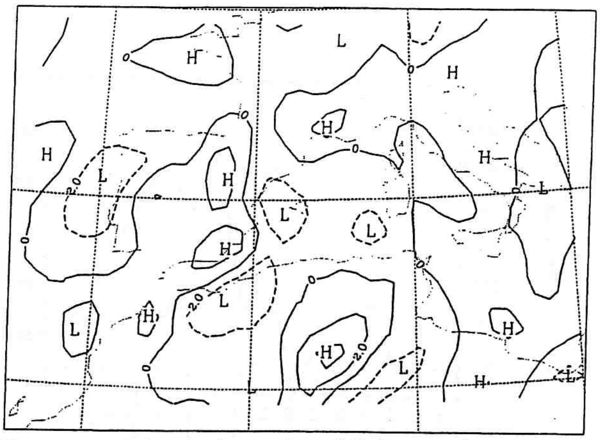

Figure 12. *Moisture divergence (full line) and convergence (dashed line) at 1000 hPa for 0000 UTC 4 October. Contour interval is 2 mg m^{-2} s^{-1} hPa^{-1}.*

3.4. Composite charts

In order to summarize the information obtained from the diagnosis of LAM analyses, a composite chart was created by plotting the zero lines of vertical quasi-geostrophic forcing at 850 hPa, the θ_e difference between 500 and 1000 hPa and the moisture flux convergence at 1000 hPa. These diagrams highlight where upward vertical forcing, convective instability and water vapour convergence overlap, so indicating the area where the three synoptic mechanisms become favourable for development of convection. Figure 13 shows the overlap zone at different times in the rainfall event.

(a) At 0000 UTC 2 October (Figure 13(*a*)) the zone of coincidence was very small and located in the south of Catalonia.
(b) At 0000 UTC 3 October (Figure 13(*b*)) the intersection zone was from south Catalonia and eastern Spain to North Africa, with major upward forcing over south Catalonia and the Balearic Isles.
(c) At 0000 UTC 4 October (Figure 13(*c*)) the intersection zone remained over the Western Mediterranean from Catalonia to North Africa, near current convective activity and where new convective cells continued to form.
(d) At 0000 UTC 5 October (Figure 13(*d*)) the coincidence zone continued over the Mediterranean, with major upward forcing located south of the Balearic Isles, in association with cyclogenesis and extending northward towards the gulf of Lyon.

Looking at the general evolution of the coincidence zone in the composite charts (at 0000 UTC and 1200 UTC) and locating the development of convection from satellite images (shown in the next section), we can deduce that, in this event, the composite chart

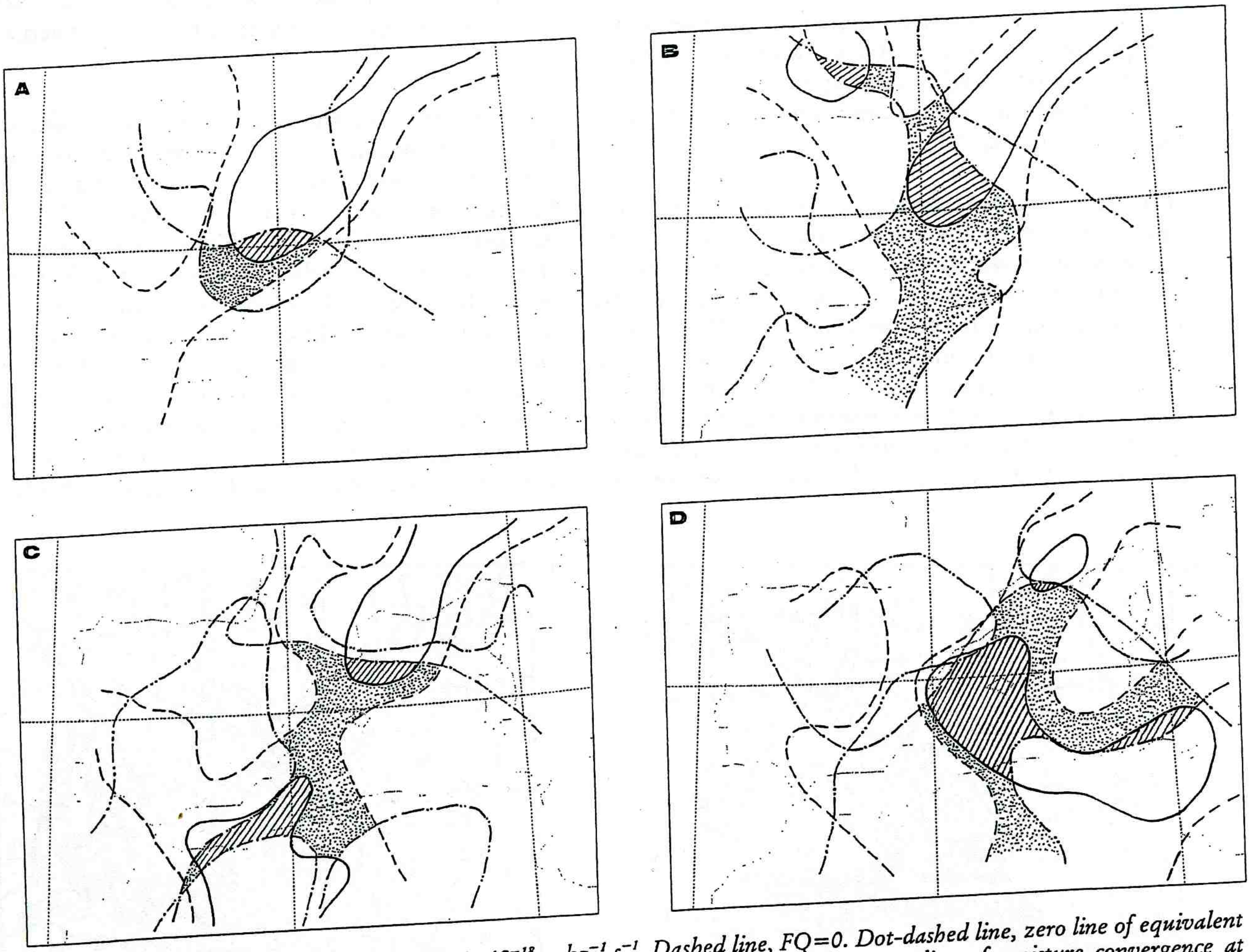

Figure 13. *Composite charts. Full line, FQ=4×10^{-18} m kg^{-1} s^{-1}. Dashed line, FQ=0. Dot-dashed line, zero line of equivalent potential temperature difference between 500 and 1000 hPa. Dot-dot-dashed line, zero line of moisture convergence at 1000 hPa. Dotted zone denotes existence of the three forcing mechanisms, and shaded zone denotes the zone of greatest vertical upward forcing.* (a) *0000 UTC 2 October,* (b) *0000 UTC 3 October,* (c) *0000 UTC 4 October and* (d) *0000 UTC 5 October.*

method gives useful information on where the probability of thunderstorm development was high.

4. Mesoscale study

The importance of scale interaction in producing heavy rainfall events has been highlighted (see Bosart, 1984 and Rockwood & Maddox, 1988, for example). Consequently, a sub-synoptic study was carried out in order to look for the focusing factors which could be responsible for triggering the convection which led to the heavy rainfall observed during this case. We also concentrated our mesoscale investigation between 0000 UTC 3 October and 0000 UTC 5 October, the period during which mesoscale phenomena were most significant and heavy rain produced the most important consequences for Catalonia.

A problem arises in the process of mesoscale analysis as a consequence of the lack of data available over the sea. In order to overcome this inconvenience, conceptual models of pressure distribution around a thunderstorm as indicated by, for example, Fujita (1986) and Schofield & Purdom (1986), together with Meteosat imaginary, have been used. Moreover, pressure dipole structures (high pressure in the windward side and low in the lee) developed by a mountain range when wind blows perpendicular to it have been taken into account, particularly for southerly flows in the Alps (Vergeiner *et al.*, 1982), the Pyrenees (Bessemoulin *et al.*, 1993) and the Atlas Mountains (Jansá *et al.*, 1986).

In the series of six-hourly hand-made surface mesoanalyses (only partially reproduced in this paper; Figure 14) covering Eastern Spain, North Africa, Southern France and the Western Mediterranean, some mesoscale structures were present during the entire episode. The role of these varied at different times during the event. The first mesoscale feature was the orographically induced Algerian surface low (identified as La in Figure 14), located on the lee side of the Atlas Mountains, which was only weakly present in the objective analysis, but is clearly depicted in the mesoscale charts. The second important and stationary structure, near the Catalonian coast, was a mesohigh created at the windward side of the Pyrenees (identified as Hp) and finally there was the mesohigh (identified as Ha) in the windward of the Alps. Both of the latter were as a consequence of the blocking action on the large-scale flow. These structures constituted the basic mesoscale configuration as a consequence of the persistence of a northward flow for several days. Moreover, throughout the period a high water vapour content over the Mediterranean was also present, with dew point values between 18°C and 23°C.

The first convective cells appeared on 2 October in the afternoon over the Iberic mountains (inland of Spain). These were caused by diurnal heating within the air mass advected from the west by the Atlantic low, and they were transported towards the coast. Most of this convection fell in the evening, but the merging of some convective cells created the first MCS over the coast (labelled a in Figure 15(*a*)), reinforced and fed by the convergence between the outflow from the Pyrenean mesohigh and the humid south-eastern flow over the sea. Thus, during the night, most convective activity was triggered and located over the sea, but close to the coast of Catalonia, and related to the same convergence line.

The convective activity over the sea was maintained during the morning of 3 October, but new cells developed progressively between Catalonia and the Balearic Isles (cells b and c in Figure 15(*b*)). The mesoanalysis on 1200 UTC (Figure 14(*a*)) shows the Pyrenean mesohigh, which extended its influence to the south, towards the more humid air, due to the outflow boundary of the convective system c. This was due to the new cell d (see Figure 15(*c*)), which grew and reached that size in half an hour. Later, this new system drifted to Catalonia (where some showers were observed, see Figure 4) and to the South of France, by the winds at medium levels, and continued its displace-

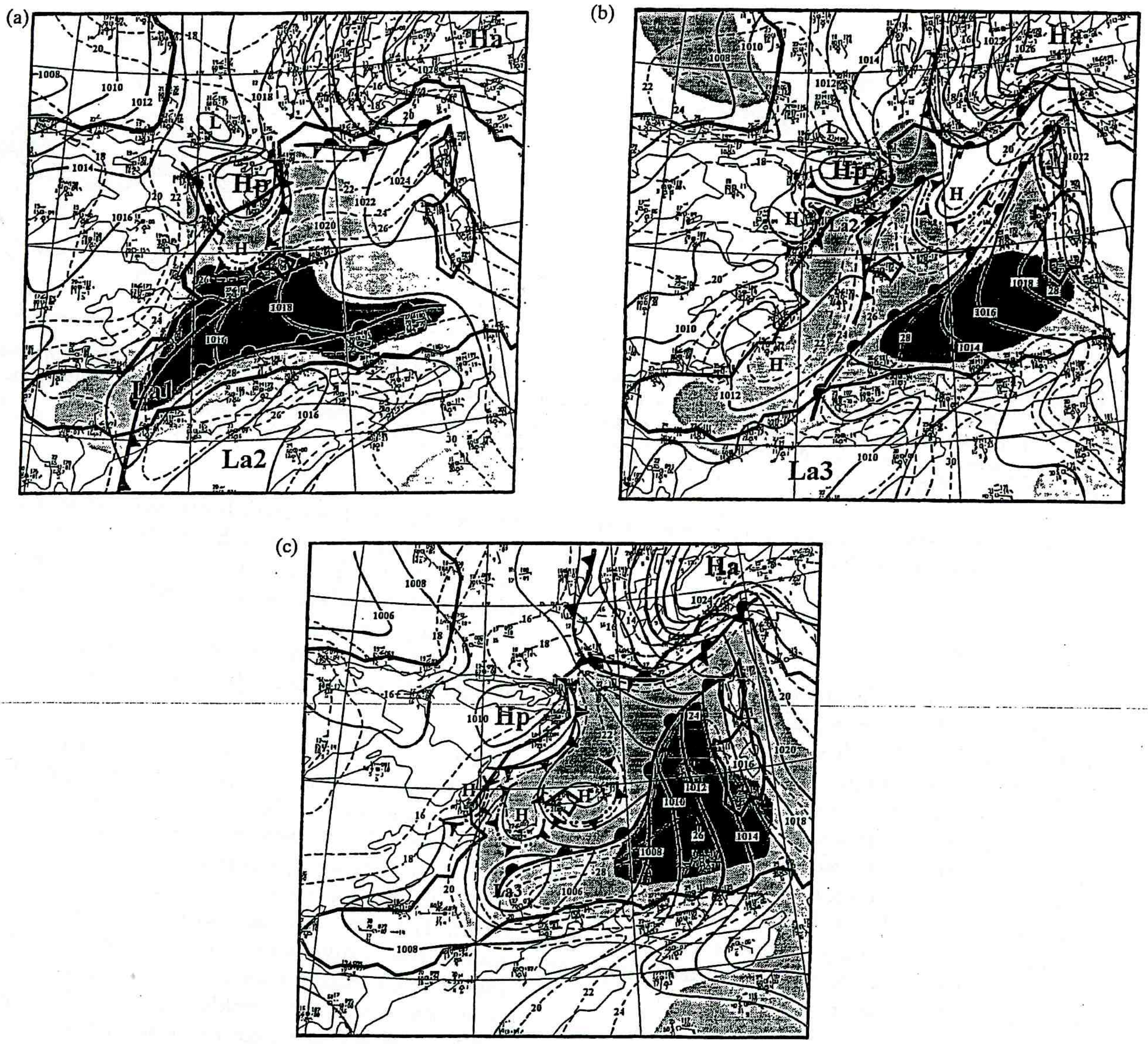

Figure 14. *Surface hand analysis at (*a*) 1200 UTC 3 October, (*b*) 1200 UTC 4 October and (*c*) 0000 UTC 5 October. Full lines are isobars plotted with an interval of 2 hPa. Dashed lines, isotherms with an interval of 2°C. Shaded zones represent areas with dew point greater than 18°C and 22°C. The thick line indicates the coastline.*

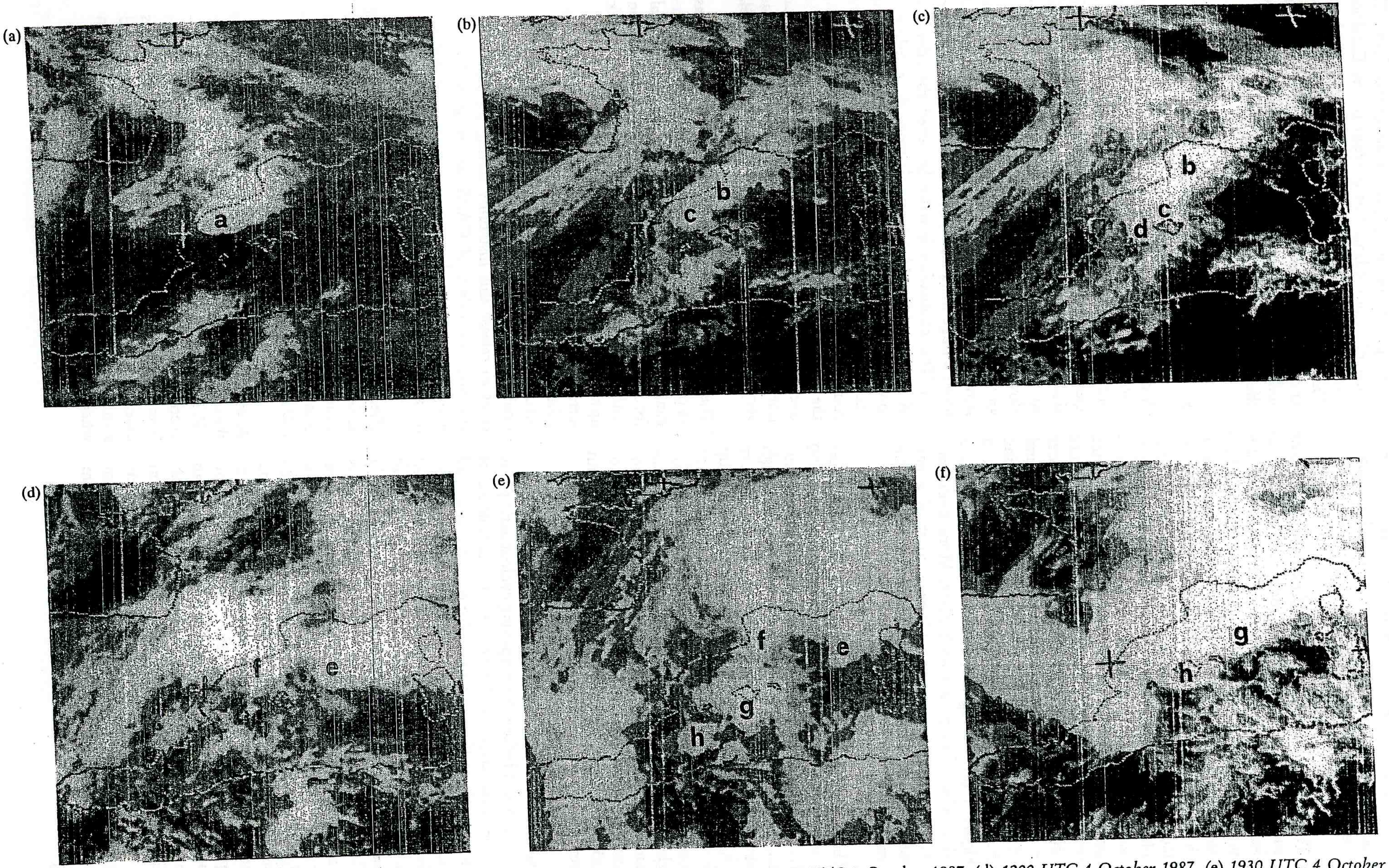

Figure 15. *IR Meteosat image for* (a) *0130 UTC 3 October 1987,* (b) *1030 UTC 3 October 1987,* (c) 1200 UTC 3 October 1987, (d) *1200 UTC 4 October 1987,* (e) *1930 UTC 4 October 1987 and* (f) *0130 UTC 5 October 1987. Labels indicate convective cells referenced in the text.*

ment toward the east fed by the stationary front between the cold air from the Alps mesohigh and the warm Mediterranean air.

The mesoscale situation remained quite stationary with successive developments of new convective cells between Catalonia and the Balearic Isles, partially due to the stationary convergence line related to the Pyrenees and partially by the northward displacement of the Algerian low La2 into the Mediterranean. The surface mesoanalysis at 1200 UTC 4 October (Figure 14(*b*)) reflects the fact that the most important convective cells seem to be connected to the Pyrenean convergence line and to the warm and stationary fronts in the north-east of the Balearic Isles (cells e and f in Figure 15(*d*)). At that time, there was another heavy shower in Barcelona. Fronts associated with the La2 low and the action of outflow boundaries from pre-existing thunderstorms developed new convective cells (g, h in Figure 15(*e*)) during the afternoon over the Balearic Isles, where heavy rain took place. More significant was the presence over the Algerian coast of a new mesolow La3, which deepened and moved towards the sea.

The evolution of the La3 low during the next hours was very important. Figure 14(*c*) (mesoanalysis at 0000 UTC 5 October) shows the low over the Mediterranean where there was generalized convection, although some cells can be identified by continuity (Figure 15(*f*)). The structure of convergence lines produced by the mesohighs Ha and Hp still remained. The low La3 continued its displacement to the north very rapidly, releasing the intrusion of cold air over the Mediterranean from Spain, helped probably by the cold air downdrafts from the convective cells. The displacement of La3 to the north represents the end of the heavy rain event.

The mesoscale evolution at the time of maximum precipitation and before the deepening cyclogenetic phase can be summarized as follows. As a consequence of the synoptic configuration established and maintained since the preceding days, the dominant southerly winds crossed the Atlas Mountain range and produced the surface Algerian low. This constitutes the 'shallow' orographic cyclogenesis phase, which is not properly reflected in the objectively analysed charts, but is clearer in the hand mesoscale analyses. Due to the slow movement of the European anticyclone, the low helped the development of the easterly and south-easterly flow in the Mediterranean. The warm and humid Mediterranean air reached the coast of Spain, in particular the Catalonia coast. Although forcing by orographic lifting at the coastal mountain ranges can contribute to the final intensity of the rain in the Catalonian coastal zone, in this case the main mechanism for trigger convection probably was the low-level convergence provided by the encounter between the warm air over the sea and the outflow coming mainly from an orographic mesohigh (the Pyrenean mesohigh). This took place not inland, but in front of the Catalonian coast, where most of the convective activity began. This fact is apparent even from the synoptic analyses and the spatial distribution of θ_e at 1000 hPa, which indicate strong quasi-stationary low-level forcing over the region and the juxtaposition of two air masses.

5. Summary and conclusions

A description of a deep moist convective event which produced floods in the Catalonian region of Spain has been presented. At the synoptic scale, the meteorological pattern can be characterized by a cyclonic circulation throughout the troposphere, which was initially to the north-west of Spain and which moved very slowly to lower latitudes. The surface pattern reveals an anticyclone over central Europe which moved slowly south-eastwards, while at middle and upper levels a ridge was located over the western Mediterranean. This circulation initially favoured the advection of warm and humid Atlantic air from the south-west toward the eastern Iberian peninsula; later, very warm and humid Mediterranean air was advected from the south-east in a shallow layer near the surface. During the entire episode the temperature in the troposphere over the western Mediterranean was higher than normal for this time of year, and the humidity was very high up to 500 hPa, and very low above this level.

The upward quasi-geostrophic vertical forcing was important at low levels over the western Mediterranean, but not at 500 hPa, where the stronger vertical forcing remained over western Spain in association with the Atlantic cyclone. Nevertheless, a weak upward forcing over Catalonia and the western Mediterranean was present. Analysis of the regional atmospheric stability indicated that there was convective instability over the western Mediterranean and, in particular, over the Spanish coast. Weak ascent was sufficient to release this instability during the heavy rain episode. The values of CAPE and bulk Richardson number show that the environment was appropriate for supporting convection.

There was a high moisture content. Convergence of moisture at 1000 hPa was observed over the area of thunderstorm development, providing better guidance than the integrated values for the 1000–850 and 1000–700 hPa layers.

A composite chart which highlighted the area where there was quasi-geostrophic upward forcing at 850 hPa, moisture convergence at 1000 hPa and convective instability between 1000 and 500 hPa deduced from objective analysed fields has been found, in this case, to be an effective tool to determine the broad area where forecasters must concentrate their attention when looking for mesoscale focusing mechanisms.

Surface mesoscale analysis indicated that three main structures were present during the whole episode. An Algerian low in the lee of the Atlas Mountains, a mesohigh over Catalonia in the windward side of the Pyrenees and a mesohigh in the windward side of the Alps. The quasi-stationary convergence line located over the sea and near the Catalonian coast was the most-effective focusing mechanism; it was there where most convective cells developed. During the final stages of the event a cyclogenetic process over the Algerian sea was the principal source of convergence, but this cyclogenesis also transported older and dryer air into the region and ended the rainfall event.

The Catalonian topography could perhaps contribute to the final intensity of the rain in the coastal zone, since the height of the coastal range is enough to lift the air to its level of free convection. Moreover, the land–sea discontinuity could produce a sharp change in surface roughness, providing a secondary convergence zone with a strong influence on a potentially unstable air mass like the one observed in this case over the western Mediterranean.

The importance of interaction between the synoptic-scale environment and the mesoscale focusing mechanism can be seen from the comparison of Figure 13 and Figure 14. The large scale creates an environment favourable for the development of thunderstorms near Catalonia. The orography creates meso-alpha-scale circulations in the lee and windward sides of the range mountains, and these produce meso-beta convergence zones which, when located within the broad area where the large scale is favourable for thunderstorm development, trigger the convection as isolated cells.

For the past four years, a McIdas system (Suomi *et al.*, 1983) has been operated by the INM of Spain. Analysis and forecast products from the LAM as well as derived fields are now available for the forecasters in near real time and composite charts similar to those presented here can be built in the forecast offices. Although mesoscale hand analyses are routinely made in the INM, this case study shows the importance of sub-synoptic analysis, especially in regions such as the Mediterranean Sea where there is a lag of data and where orography can significantly perturb the large-scale circulation.

Although this research adds information to previous studies on the synoptic frame from derived fields, the general scenario is quite similar to other cases of heavy rain which have occurred not only in Catalonia but also in eastern Spain. More research has to be done to identify favourable synoptic environments and focusing mechanisms to obtain more-discriminating guidance for the identification of the area of major rainfall. In addition, numerical experiments can help to identify physical and dynamical mechanisms involved in this type of convective event.

Acknowledgements

The authors acknowledge S. Alonso for his continuous comments and suggestions during the development of this study, M. Pedder for his comments on the original manuscript and D. Gomis for his help in the filtering process of the fields. This research has been partially sponsored by the DGICYT of Spain under project PB89–0428 and by the EC under contract EV5V-CT92–0167.

References

Alonso, S. & Puigcerver, M. (1978). On the energetics of levante storms. *Arch. Meteorol. Geophys. Bioklimatol.*, **A-27:** 105–116.

Barnes, S. L. (1985). Omega diagnosis as a supplement to LFM/MOS guidance in weakly forced convective situations. *Mon. Wea. Rev.*, **113:** 2122–2141.

Barnes, S. L. & Newton, C. W. (1986). Thunderstorms in the synoptic setting. In *Thunderstorm. Morphology and Dynamics*, 2nd edn. (E. Kessler, editor), 75–112. University of Oklahoma Press.

Benet, C. (1986). *Meteorological Data in Sabadell 1897–1979.* (In Catalan). Ajuntament de Sabadell.

Bessemoulin, P., Bougeault, P., Genovés, A., Jansà, A. & Puech, D. (1993). Mountain pressure drag during PYREX. *Beitr. Phys. Atmosph.*, **66:** 305–325.

Bosart, L. F. (1984). The Texas coastal rainstorm of 17–21 September 1979: an example of synoptic–mesoscale interaction. *Mon. Wea. Rev.*, **111:** 1108–1133.

Caracena, F. & Fritsch, J. M. (1983). Focussing Mechanism in the Texas hill country flash floods of 1978. *Mon. Wea. Rev.*, **111:** 2319–2332.

Diaz-Pabón, R. (1988). *Three-dimensional Meteorological Fields Analysis Operative in the INM.* (In Spanish.) INM Serie A.

Doswell, C. A. III (1987). The distinction between large-scale and mesoscale contribution to severe convection: a case study example. *Wea. Forecasting*, **2:** 3–16.

Durran, D. R. & Snellman, L. W. (1987). The diagnosis of synoptic-scale vertical motion in an operational environment. *Wea. Forecasting*, **2:** 17–31.

Elsner, J. B., Drag, W. H. & Last, J. K. (1989). Synoptic weather patterns associated with Milwaukee, Wisconsin flash flood of 6 August 1986. *Wea. Forecasting*, **4:** 537–554.

Font, I. (1983). *Climatology of Spain and Portugal.* (In Spanish.) INM. Madrid. 296 pp.

Fujita, T. T. (1986). Mesoscale classifications: their history and their application to forecasting. In *Mesoscale Meteorology and Forecasting* (Ray, P. S., editor), 18–35. American Meteorological Society.

García-Dana, F., Font, R. & Rivera, A. (1982). *Meteorological Situation During the Heavy Rain Event in the Eastern Zone of Spain during October-82.* (In Spanish.) INM.

Gomis, D. & Alonso, S. (1988). Structure function responses in a limited area. *Mon. Wea. Rev.*, **116:** 2254–2264.

Hoskins, B. J. & Pedder, M. A. (1980). The diagnosis of middle latitude synoptic development. *Q. J. R. Meteorol. Soc.*, **106:** 707–719.

Iribarne, J. V. & Godson, W. L. (1981). *Atmospheric Thermodynamics.* 2nd edn. Reidel Publishing. 259 pp.

Jansá, A., Ramis, C. & Alonso, S. (1986). The Mediterranean thunderstorm on 15 November 1985: triggering mechanism. (In Spanish.) *Rev. Meteorol.*, **8**: 7–19.

Llasat, M. C. (1987). *Heavy Rain Events in Catalonia: Genesis, Evolution and Mechanism.* (In Spanish.) Univ. de Barcelona Press.

McGinley, J. (1986). Nowcasting mesoscale phenomena. In *Mesoscale Meteorology and Forecasting*. (Ray, P. S., editor), 657–688. American Meteorological Society.

O'Brien, J. J. (1970). Alternative solutions to the classical vertical velocity problem. *J. Appl. Meteorol.*, **9**: 197–203.

Ramis, C. (1976). *Contribution to the Upper Air Climatology in Mallorca.* (In Spanish.) Univ. de Barcelona.

Riosalido, R. (1990). Satellite characteristics of mesoscale convective systems over Spain. *Proceedings of the Eighth Meteosat Scientific Users Meeting. Norrkoping. EUMETSAT EUMPO8*, 127–130.

Rockwood, A. A. & Maddox, R. A. (1988). Mesoscale and synoptic scale interactions leading to intense convection: the case of 7 June 1982. *Wea. Forecasting*, **3**: 56–68.

Schwartz, B. E., Chappel, C. F., Togstad, W. E. & Zhong, Xiao-Ping, (1990). The Minneapolis flash flood: meteorological analysis and operational response. *Wea. Forecasting*, **5**: 3–21.

Scofield, R. A. & Purdom, J. F. W. (1986). The use of satellite data for mesoscale analyses and forecasting applications. In *Mesoscale Meteorology and Forecasting* (Ray, P. S., editor), 118–150. American Meteorological Society.

Show-Jun Chen, Le Sheng Bai & Barnes, S. L. (1988). Omega diagnosis of a cold vortex with severe convection. *Wea. Forecasting*, **3**: 296–304.

Suomi, V., Fox, R., Limaye, S. & Smith, W. (1983). McIDAS III: a modern interactive data access and analysis system. *J. Appl. Meteorol.*, **22**: 766–778.

Vergeiner I., Steinacker, R. & Dreiseitl, E. (1982). The south foehn case 4/5 May 1982. In *Alpex Preliminary Scientific Results* (Kuettner, J. P., editor), 143–154. GARP-ALPEX n 7, WMO.

Weisman M. L. & Klemp, J. B. (1986). Characteristics of isolated convective storms. In *Mesoscale Meteorology and Forecasting*, (Ray, P. S., editor), 331–358. American Meteorological Society.